ON THE LOADSHARE BETWEEN NAILING AND BONE

Paulo Pedro Kenedi[1], paulo.kenedi@cefet-rj.br
José Renato de Oliveira e Silva Neto[1], netoengemec@yahoo.com.br
Rodrigo Ribeiro Pinho Rodarte[1,2], rrodarte@globo.com

[1]Programa de Pós-graduação em Engenharia Mecânica e Tecnologia de Materiais –PPEMM -CEFET/RJ – Av. Maracanã, 229, RJ, Brazil.
[2]Instituto Nacional de Traumatologia e Ortopedia – INTO -Av. Brasil, 500, RJ, Brazil.

Abstract. *Intramedullary nailing, which is positioned inside a long bone as a human femur, has been used to fix fractured bones during healing process, sharing the mechanical loads with bone. An analytical model, based in mechanics of solids, is presented to describe, at diaphyseal cross section, the load share between bone and nailing. Also, an elastic finite element model is provided as a reference. The results show a good correspondence between models.*

Key words*: intramedullary nailing, load share, analytical model*

1. INTRODUCTION

Intramedullary nailing, for now on called nailing, has been used to stabilize fractured bones and to shorten the patient recovery time, through the load share between bone and nailing. Many researchers have been spending efforts to describe aspects of biomechanical performance of skeletal systems, trying to understand how gait patterns can affect the load distribution in human femurs, as Bergmann *et al*. (2001) and Duda *et al*. (1997),which have published interesting articles. Other researches concentrated the influence of muscle forces in the development of the stress distribution in human femurs, as in Kenedi and Riagusoff (2015) and Duda *et al*. (1998). Also a more detailed stress analysis for human femur and ostheosynthesis systems were addressed in Doblaré *et al*. (2004), Kenedi and Vignoli (2017), Kenedi and Vignoli (2016) and Taylor *et al*. (1996).

2. ANALYTICAL MODEL

To model the relation of external forces acting at proximal human femur and the internal loads acting in a human bone/nailing set at a diaphyseal cross section, an analytical model is proposed by the utilization of mechanics of solids theory. The analytical calculations are presented and compared with a well-established finite element software, as ANSYS.

Figure 1 shows, schematically, the loading model configuration with four external static forces applied at femur's head, adapted from the Taylor's fourth load case of human left femur's head in Taylor *et al*. (1996). The external forces are named: (A) Joint Reaction - P_1, (B) Abductors - P_2, (C) Ilioopsoas - P_3 and (D) Ilio-Tibial Tract - P_4. See Bitsakos (2015) for more complete muscle loading cases description.

The analytical model supposes that cross sections, for both nailing and bone, are hollow circles. Only the cortical tissue is considered for bone and the nailing is made of stainless steel. It is supposed that all materials are isotropic and the stresses remain elastic.

2.1 Equivalent Forces and Moments

The initial step of the analytical model consist in rewriting the external forces, shown in Fig. 1.a in a equivalent set of forces and moments at the cross section 1 centroid (see Fig.1.b), as shown in sequence:

$$P_i = P_i^x \vec{i} + P_i^y \vec{j} + P_i^z \vec{k} \qquad d_i = d_i^x \vec{i} + d_i^y \vec{j} + d_i^z \vec{k} \tag{1}$$

$$\begin{pmatrix} V_i^x \\ V_i^y \\ V_i^z \end{pmatrix} = \begin{pmatrix} P_i^x \\ P_i^y \\ P_i^z \end{pmatrix} \qquad \begin{pmatrix} M_i^x \\ M_i^y \\ M_i^z \end{pmatrix} = \begin{pmatrix} d_i^y P_i^z - d_i^z P_i^y \\ d_i^z P_i^x - d_i^x P_i^z \\ d_i^x P_i^y - d_i^y P_i^x \end{pmatrix} \tag{2}$$

Where, $\vec{i}$, $\vec{j}$ and $\vec{k}$ are the unit vectors. The index i ranges from 1 to 4, because the four external forces. P_i and d_i are, respectively, the external forces and the distances between each force application point and the set cross section 1 centroid.

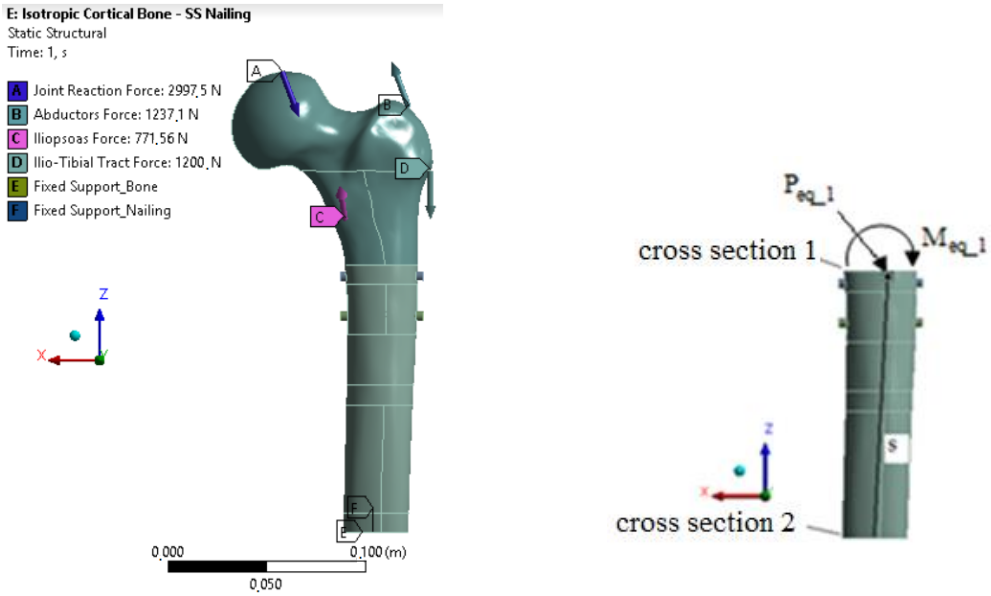

(a) (b)

Figure 1.(a) External forces and (b) Equivalent force and moment at cross section 1.

The sum of forces (V_x, V_y, V_z) and the sum of moments (M_x, M_y, M_z)that are acting at the set cross section 1 centroid are:

$$V_{x\_1} = \sum_{n=1}^{4} V_i^x \qquad V_{y\_1} = \sum_{n=1}^{4} V_i^y \qquad V_{z\_1} = \sum_{n=1}^{4} V_i^z \tag{3}$$

$$M_{x\_1} = \sum_{n=1}^{4} M_i^x \qquad M_{y\_1} = \sum_{n=1}^{4} M_i^y \qquad M_{z\_1} = \sum_{n=1}^{4} M_i^z \tag{4}$$

$$P_{eq\_1} = V_{x\_1}\,\vec{i} + V_{y\_1}\,\vec{j} + V_{z\_1}\,\vec{k} \qquad M_{eq\_1} = M_{x\_1}\,\vec{i} + M_{y\_1}\,\vec{j} + M_{z\_1}\,\vec{k} \tag{5}$$

To estimate the equivalent force and moment that are acting at the cross section 2, an additional step has to be taken:

$$\begin{pmatrix} V_x \\ V_y \\ V_z \end{pmatrix} = \begin{pmatrix} V_{x\_1} \\ V_{y\_1} \\ V_{z\_1} \end{pmatrix} \qquad \begin{pmatrix} \mathrm{M_x} \\ \mathrm{M_y} \\ \mathrm{M_z} \end{pmatrix} = \begin{pmatrix} \mathrm{s^y V_{z\_1} - s^z V_{y\_1} + M_{x\_1}} \\ \mathrm{s^z V_{x\_1} - s^x V_{z\_1} + M_{y\_1}} \\ \mathrm{s^x V_{y\_1} - s^y V_{x\_1} + M_{z\_1}} \end{pmatrix} \tag{6}$$

$$P_{eq} = V_x\,\vec{i} + V_y\,\vec{j} + V_z\,\vec{k} \qquad M_{eq} = M_x\,\vec{i} + M_y\,\vec{j} + M_z\,\vec{k} \tag{7}$$

Where *s* is the distance between the centroids of cross sections 1 and 2.

2.2 Stiffnesses and load share calculations

The stiffnesses calculations use the bone and nailing part between cross sections 1 and 2. The bone partis modeled as a generic frustum of a hollow cone and the nailing is modeled as a hollow cylinder.

Figure 2.a shows a generic cross section at *z* coordinate. Note that it is supposed that the nailing and the bone are in a perfectly concentric fashion. Figure 2.b shows the lateral view of bone diaphyseal part, between cross sections 1 and 2.The bone and the nailing are considered to be in parallel configuration, so the transversal displacements and slopes must be the same.

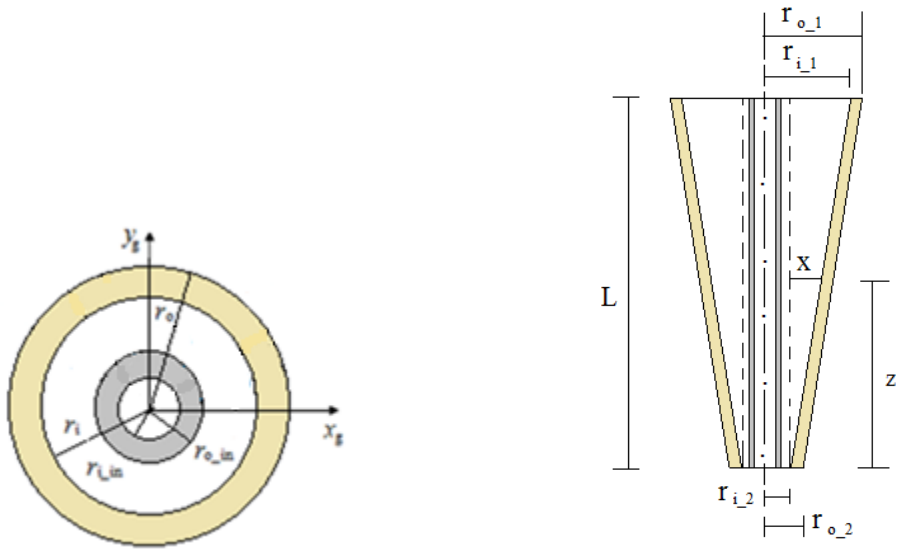

(a) (b)

Figure 2. (a)Nailing and bone cross sections at a vertical coordinate and (b) longitudinal cut of bone/nailing set.

Where the indexes $_i$ and $_o$ means, respectively, inner and outer, the indexes $_b$, and $_{in}$ means, respectively, bone and nailing and r is a radius. The Table 1 shows the expressions used to implement the stiffnesses calculations. Note that some cross section variables are also available in Appendix. Table 2 is used to estimate the load share at cross section 1, as in Crandall *et al*. (1978):

Table 1. Bone/nailing stiffnesses.

	bone	nailing
Axial	$k^b_{ai} = \left(\int_0^L \frac{1}{A^b(z)E^b} dz \right)^{-1}$	$k^{in}_a = \frac{A^{in}E^{in}}{L}$
Bend x axis	$k^b_{bx} = \left(\int_0^L \frac{1}{I^b_x(z)E^b} dz \right)^{-1}$	$k^{in}_{bx} = \frac{I^{in}_x E^{in}}{L}$
Bend y axis	$k^b_{by} = \left(\int_0^L \frac{1}{I^b_y(z)E^b} dz \right)^{-1}$	$k^{in}_{by} = \frac{I^{in}_y E^{in}}{L}$
Shear x axis	$k^b_{sx} = \left(\int_0^L \frac{1}{I^b_x(z)E^b} dz \right)^{-1}$	$k^{in}_{sx} = \frac{I^{in}_x E^{in}}{L}$
Shear y axis	$k^b_{sy} = \left(\int_0^L \frac{1}{I^b_y(z)E^b} dz \right)^{-1}$	$k^{in}_{sy} = \frac{I^{in}_y E^{in}}{L}$
Torsion	$k^b_t = \left(\int_0^L \frac{1}{J^b(z)G^b} dz \right)^{-1}$	$k^{in}_t = \frac{J^{in}G^{in}}{L}$

Table 2. Bone/nailing forces and moments share.

	bone	nailing
Axial	$V^b_{z\_1} = \frac{k^b_a}{k_{a\_eq}} V_{z\_1}$	$V^{in}_{z\_1} = \frac{k^{in}_a}{k_{a\_eq}} V_{z\_1}$
Bend x axis	$M^b_{bx\_1} = \frac{k^b_{bx}}{k_{bx\_eq}} M_{x\_1}$	$M^{in}_{bx\_1} = \frac{k^{in}_{bx}}{k_{bx\_eq}} M_{x\_1}$
Bend y axis	$M^b_{by\_1} = \frac{k^b_{by}}{k_{by\_eq}} M_{y\_1}$	$M^{in}_{by\_1} = \frac{k^{in}_{by}}{k_{by\_eq}} M_{y\_1}$
Shear x axis	$V^b_{x\_1} = \frac{k^b_x}{k_{x\_eq}} V_{x\_1}$	$V^{in}_{x\_1} = \frac{k^{in}_x}{k_{x\_eq}} V_{x\_1}$
Shear y axis	$V^b_{y\_1} = \frac{k^b_y}{k_{y\_eq}} V_{y\_1}$	$V^{in}_{y\_1} = \frac{k^{in}_y}{k_{y\_eq}} V_{y\_1}$
Torsion	$M^b_{z\_1} = \frac{k^b_t}{k_{t\_eq}} M_{z\_1}$	$M^{in}_{z\_1} = \frac{k^{in}_t}{k_{t\_eq}} M_{z\_1}$

Where each equivalent stiffness k_{eq} is calculated by the sum of bone and nailing stiffnesses. For instance, the equivalent axial stiffness is calculated as: $k_{a\_eq} = k^b_a + k^{in}_a$. The elastic modulus of the nailing E^{in} is constant, but the elastic modulus of the bone E^b is not, so it is used a average value available in technical literature, as Doblare *et al*. (2004). Note that the cross section goemetric parameters of bone as area $A^b(z)$, area moment of inertia $I^b(z)$ and polar area moment of inertia $J^b(z)$ varies with thevertical coordinate z are available in Tables 3 and 4.

To estimate the load share in cross section 2 the equations (7) must be usedwith Table 2 results.

3. NUMERIC MODEL

The finite element software ANSYS 16 was used as a reference to evaluate the analytical model performance. The forces applied are shown in Fig. 1.a. The bone was modeled as linear, elastic and isotropic, with E^b = 20 GPa, G^b = 8.05 GPa, ν^b = 0.236. The nailing was modeled as elastic behavior, with E^{in} = 193GPa, G^{in} = 73.6GPa, ν^{in} = 0.31, as in Kenedi and Vignoli (2016).

The four external forces components are (N): P_1 = (–1,062; -130; -2,800), P_2 = (430; 0; 1,160),P_3 = (78; 560; 525) and P_4 = (0; 0; -1,200). The distances between forces point of application and the set cross section 1centroid are (mm): d_1 = (47; -12; 97.6), d_2 = (-17; -15; 79.6), d_3 = (15; -38; 23.6) and d_4 = (-28; -13; 47.6).The vertical distance (z) between cross sections 1 and 2 is 135.4 mm. The cross section bone geometry is defined by r_{o_1} = 17.55 mm, r_{i_1} = 11.05 mm, r_o = 13.75 mm, r_i = 6.88 mm, and the cross section intramedullary nailing is defined by r_{o_in} = 5 mm (d_{o_in}= 10 mm external diameter) and r_{i_in} = 2.5 mm. Figure 3 shows the utilized mesh and cross sections 1 and 2.

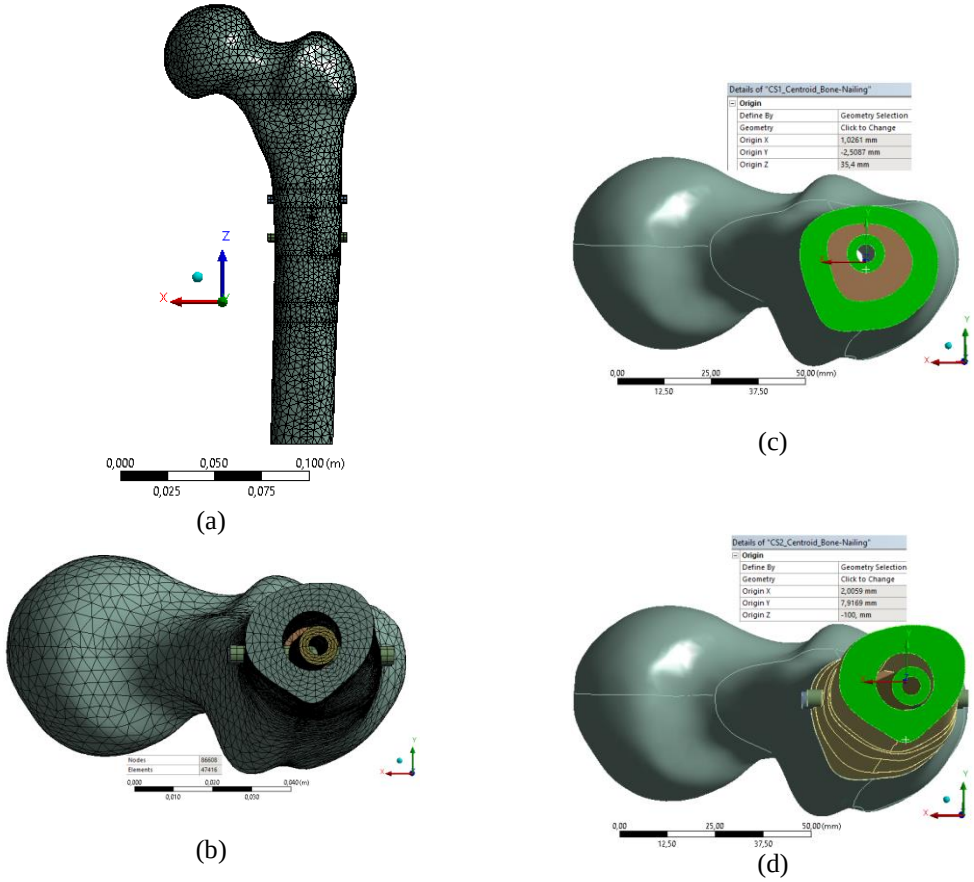

Figura 3. Mesh (a) lateral view (b)transversal view at cross section 2. Cross sections: (c) 1 and (d) 2**.**

A 2.0 mm mesh was generated for bone and nailing, after a convergence study.47416 solid elements (SOLID185, SOLID186 and SOLID187) and contact elements (CONTA174 and TARGE170) were used, as well 86608 nodes.

4. RESULTS

Both results, for analytical and numeric models, are presented in this section. Figure 4 shows the numeric results from ANSYS 16 software and in Fig. 5 shows a comparison between analytical and numeric results. In Fig. 4 the F.E. numeric model outputs are presented, showing the reactions forces and moments of a diaphyseal region obtained at the cross section 2. In Fig 5. shows the force share for transversal forces (V_x and V_y), where the bone parcel is more significative than the nailing one, while for axial force (V_z) the distribution between bone and nailing is quite equitable. The moments share shows that for cross section moments (M_x and M_y) the bone parcel is more significative than the nailing one, while the torcional moment (M_z) is quite small.

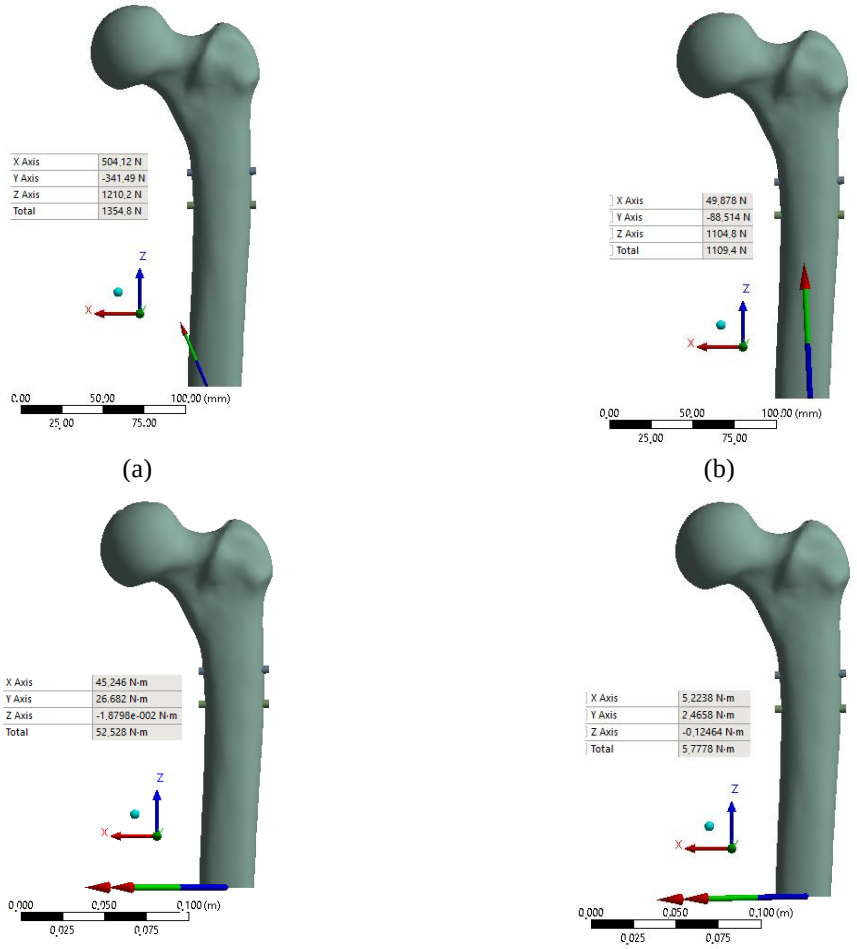

(a) (b)

(c) (d)

Figura 4. Finite Element results:Forces (a) bone and (b) nailing; Moments (c) bone and (d) nailing.

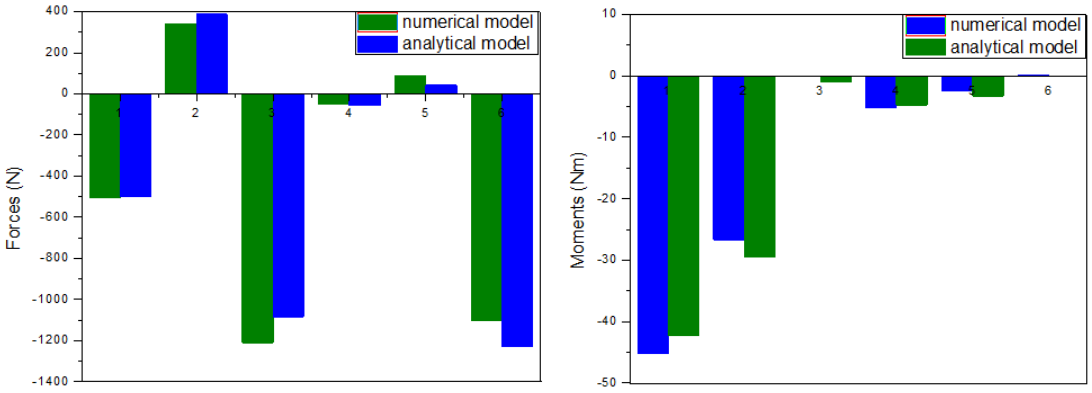

(a) (b)

Figura 5. Models results comparison: (a) forces and (b) moments.

Note that in Fig.5 the sequential numeration below the horizontal axis are: 1: V_x^b, 2: V_y^b, 3: V_z^b, 4: V_x^{in}, 5: V_y^{in} and 6: V_z^{in}; and for the Fig.5.b equivalently: 1: M_x^b, 2: M_y^b, 3: M_z^b, 4: M_x^{in}, 5: M_y^{in} and 6: M_z^{in}. The analytical model has a quite good performance when compared with numerical model, based in commercial F.E. software. The variations of cross section areas of cortical bone, in function of *z* coordinate, does not contribute to the performance of the analytical model. One possibility to improve the analytical model performance is to divide the frustum cone in more parts, to better follow the excessive variability of cortical bone cross sections.

5. CONCLUSIONS

A mechanics of solids approach was used to implement a simplified analytical model to access the load sharing between bone and nailing considering a diaphyseal set cross section of a human femur. The obtained analytic model results, when compared to the F.E. numerical model, used as reference, generated maximum differences around 10%, for both major forces and moments, in bone and nailing.

For this bone/nailing model (with the no lateral contact of bone and nailing), for the given loading, resulted in larger forces in longitudinal axis (z axis) for both bone and nail with comparable values. For transversal forces: at bone were around one third of the longitudinal bone force and at nailing were even smaller, Moments results showed that M_x and M_y for bone were larger than the M_x and M_y for nailing. The torcional moments M_z were insignificant for both, bone and nailing.

6. REFERENCES

BERGMANN, G., DEURETZBACHER, G, HELLER, M, GRAICHEN, F., ROHLMANN, A., STRAUSS, J. and DUDA, G.N. Hip contact forces and gait patterns from routine activities. **J.Biomech.**, Vol. 34, pp. 859-871, 2001.

CRANDALL, S.H., DAHL, N.C., LARDNER, T.J. *An introduction to the Mechanics of Solids*. Mc Graw Hill Int. Editions, .2nd Edition with SIunits,1978.

DOBLARÉ, M., GARCIA J.M., GÓMEZ, M.J.Modeling bone tissue fracture and healing: a review. **Engineering Fracture Mechanics**, Vol. 71, pp. 1809-1840, 2004.

DUDA, G.N., HELLER, M., ALBINGER, J., SHULZ, O.,SCHNEIDER, O. and CLAES, L. Influence of muscle forces on femoral strain distribution. Technical Note. **J.Biomech.**, Vol.31, pp.841-846,1998.

DUDA, G.N., SCHNEIDER, E., CHAO, E. Y. S.Internal Forces and Moments in the Femur during Walking. **J.Biomech.**, Vol. 30, No. 9, pp. 933-941,1997.

KENEDI, P.P. and VIGNOLI, L.L. An ostheosynthesis plate analytical model**. J Braz. Soc. Mech. Sci. Eng.**, Vol. 39, pp. 645-659. https://doi.org/10.1007/s40430-016-0598-3,2017.

KENEDI, P.P. and VIGNOLI, L.L. Intramedullary nailing: Analytical and Finite Element Approaches. In: PROCEEDINGS OF CBEB 2016. Foz do Iguaçu, Brazil, 2016.

KENEDI, P.P. and RIAGUSOFF, I.I.T. Stress development at human femur by muscle forces. **J Braz. Soc. Mech. Sci. Eng.,** Vol. 37, No. 1, pp. 31-43. DOI: https://doi.org/10.1007/s40430-014-0164-9.2015.

TAYLOR, M.E., TANNER, K.E., FREEMAN, M.A.R. and YETTRAN, A.R. Stress and strain distribution within the intact femur: compression or bending? ***Med. Eng. Phis***., Vol.18, nº2, pp. 122-131,1996.

7. APPENDIX

The geometric expressions for the frustum of a hollow cone, shown in Fig. 2.b, are explicited in Table 3:

Table 3. Bone cross section variables

	hollow cylinder	frustum of a hollow cone
area	$A^b = \pi\left(r_o^2 - r_i^2\right)$	$A^b(z) = \pi\left(\left(r_o + \left(\frac{r_{o\_1} - r_o}{L}\right)z\right)^2 - \left(r_i + \left(\frac{r_{i\_1} - r_i}{L}\right)z\right)^2\right)$
area moment of inertia	$I_x^b = I_y^b = \frac{\pi}{4}\left(r_o^4 - r_i^4\right)$	$I_x^b(z) = I_y^b(z) = \frac{\pi}{4}\left(\left(r_o + \left(\frac{r_{o\_1} - r_o}{L}\right)z\right)^4 - \left(r_i + \left(\frac{r_{i\_1} - r_i}{L}\right)z\right)^4\right)$
polar area moment of inertia	$J^b = \frac{\pi}{2}\left(r_o^4 - r_i^4\right)$	$J^b(z) = \frac{\pi}{2}\left(\left(r_o + \left(\frac{r_{o\_1} - r_o}{L}\right)z\right)^4 - \left(r_i + \left(\frac{r_{i\_1} - r_i}{L}\right)z\right)^4\right)$

Table 4. Nailing cross section variables

	hollow cylinder
area	$A^{in} = \pi\left(r_{o\_in}^2 - r_{o\_in}^2\right)$
area moment of inertia	$I_x^{in} = I_y^{in} = \frac{\pi}{4}\left(r_{o\_in}^4 - r_{i\_in}^4\right)$
polar area moment of inertia	$J^{in} = \frac{\pi}{2}\left(r_{o\_in}^4 - r_{i\_in}^4\right)$

8. RESPONSIBILITY NOTICE

The authors are the only responsible for the printed material included in this paper.